Four-point probe resistivity measurements of dicing damage in (1 0 0) and (1 1 1) single crystal silicon wafers*

SEUNG HYUN KIM, STEVEN DANYLUK
University of Illinois at Chicago, Department of Civil Engineering, Mechanics, and Metallurgy, PO Box 4348, MC: 246, Chicago, Illinois 60680, USA

Dicing damage in single crystal Czochralski (Cz) silicon wafers ((1 0 0) and (1 1 1) n-type) with initial resistivities of 0.057 and 13.89 Ω cm was investigated by forming grooves at room temperature with dicing blades lubricated with de-ionized water. The grooves were purposely misoriented by 10°, 20°, and 30° relative to the [1 1 0]. The groove surfaces were examined by optical microscopy and scanning electron microscopy while the subsurface deformation was examined after bevel polishing. The subsurface damage was quantified by four-point probe measurements along the groove length including the bevelled region with the probe tips straddling the groove. The results show that the resistivity varies with position along the groove. A maximum increase on the resistivity of 9.7% for the (1 0 0) and 8.0% for the (1 1 1) was formed for a dicing blade misorientation of 20°. Microscopy of the bevelled region shows that the damage is composed of microcracks: the depth is 0.122 mm for the (1 0 0) and 0.186 mm for the (1 1 1) at the 20° blade misorientation.

1. Introduction

The fabrication of electronic devices from single crystal ingots requires not only a knowledge of chemical and thermal processing but also mechanical processes such as grinding, sawing, lapping, polishing, and dicing. For example, large-scale integrated circuits are fabricated on silicon single crystal wafers which are prepared by slicing boules with abrasive wheels or strings impregnated with diamond grit. The diamond grit abrades the silicon surface and generates damage [1], therefore, the wafers must be polished in order to remove the wafering damage. Abrasion by the diamond impregnated blades induces damage such as microcracks and dislocations underneath the surface. This damage must be removed or minimized because it may be the cause of crack propagation during subsequent processing or may result in device malfunction [2].

Several studies have been performed on improving the efficiency of the sawing or dicing. One of these is the influence of environmental fluids on the cutting and deformation of the silicon [3, 4]. Fluids flush the debris, remove the heat generated due to the friction, redistribute the contact loads, and lubricate the contacting surfaces. Fluids may also absorb and, chemically and electrically, interact with the surfaces [5]. Temperature also influences the amount of plastic deformation of silicon [6]. The combined effects of load, fluid, temperature, and dopant level are the variables that are important to the deformation mode and the subsurface damage. Recently, the effect of fluids, loads, and temperature in silicon and GaAs has been studied [7, 8], but in spite of these and numerous other studies on the characterization of the dicing damage in single crystal silicon, the mechanisms by which the deformation is formed are not fully understood so that a quantitative model to predict damage is not yet available.

This paper reports on a laboratory simulation of high-speed lubricated cutting of oriented single crystal silicon wafers. Dicing grooves were formed and the damage generated by dicing was quantitatively characterized by measuring the resistivity of the diced region. The experimental results are used to characterize the dicing damage as a function of the blade misorientation. An analysis of the measurements of sheet resistance is compared with previous work on relating the size of the damage zone to the changes in resistivity.

2. Experimental procedure

Single crystal Czochralski (Cz) silicon wafers ((1 0 0) and (1 1 1) n-type) supplied by the Monsanto Electronic Materials Company were scribed and sectioned into rectangular shapes with dimensions 0.5 × 20 × 20 mm. The resistivity of the (1 0 0) and (1 1 1) samples was 0.057 and 13.89 Ω cm, respectively. Prior to mounting the samples in a fixture for dicing, each wafer was dipped in a 10 v/o hydrofluoric acid solution bath for 30 sec to remove the native oxide, rinsed

*Work supported by the US National Science Foundation, Grant No. MSM-8714491.

0022-2461/90 $03.00 + .12 © *1990 Chapman and Hall Ltd.*

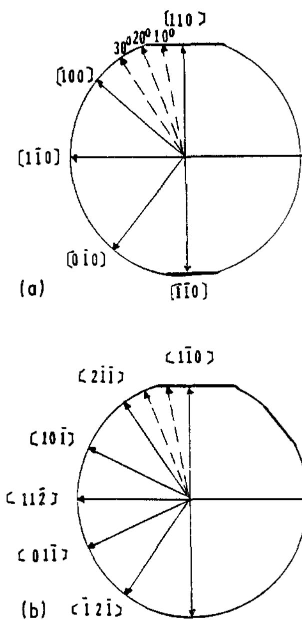

Figure 1 Schematic diagram of the crystallographic orientations in single crystal silicon wafers and the cutting directions. (a) (1 0 0) n-type, (b) (1 1 1) n-type.

in de-ionized water and immediately dried in nitrogen gas. The crystallographic orientation of the specimens is shown in Fig. 1. The dicing was done at room temperature by a diamond impregnated dicing saw-blade lubricated with de-ionized water: the dicing saw speed was 1200 r.p.m., the feed rate was 0.3 mm sec^{-1}, and the depth of the groove was 0.08 mm. Fig. 2 shows a schematic of the dicing apparatus. One groove per sample was formed and the groove orientation was adjusted to be along the [1 1 0] and at 10°, 20°, and 30° relative to the [1 1 0]. After the grooves were formed, these specimens were mounted on a 5° bevelling fixture by the use of a mounting wax. The specimens were polished with 0.012 cm alumina powder suspended in de-ionized water, followed by a two-step polish using 0.001 and 0.0005 cm alumina powder with 10 parts de-ionized water. After polishing, the specimens were etched in a modified Sirtl solution ($8\,cm^3$ HF + $16\,cm^3$ D.I. water + 2 g CrO_2) for 10 sec at room temperature in order to delineate the damage surrounding the groove which had been tapered by the bevelling.

The resistivity difference between the region containing the groove and the undamaged surface was obtained by a linear four-point probe. The measuring procedure followed ANSI/ASTM F84-73 [9]. The

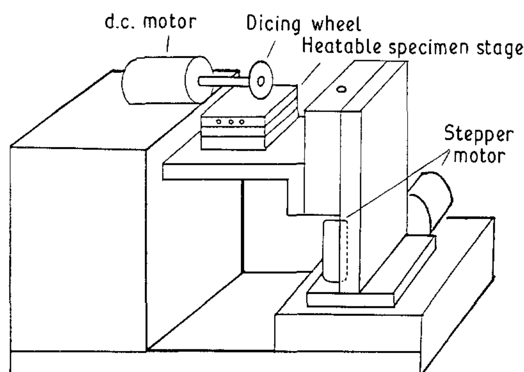

Figure 2 Schematic diagram of the dicing apparatus.

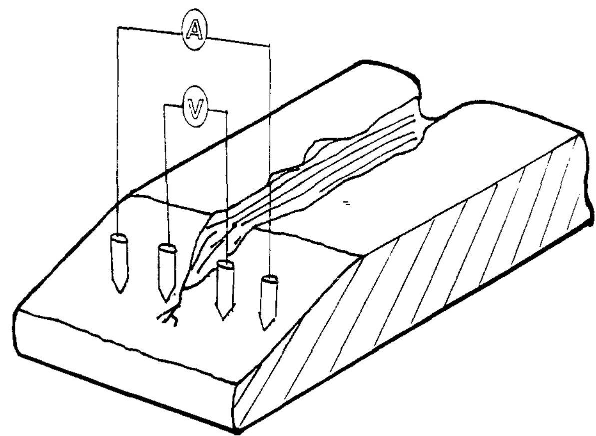

Figure 3 Schematic diagram of the four-point technique for the bevelled specimen.

specimens were positioned on the probe station such that the probes straddled the groove at the midpoint of the longitudinal axis of the specimen, and resistivity measurements were made from the edge of the bevelled region along the length of each groove (Fig. 3). Measurements were also made in regions of the specimen with similar geometry that did not contain the groove but had an identically tapered surface, and the relative change in resistivity of the diced region with each different crystallographic cutting direction to the undiced region was determined. The resistivity measurements were statistically analysed.

3. Experimental results and discussion

Fig. 4 shows the typical surface morphology of a groove of the (1 0 0) n-type silicon samples for the groove oriented along the [1 1 0] and the misorientation angles: 10°, 20°, and 30°. These optical micrographs show that the intersection of the groove wall with the surface is composed of microcracks. The conchoidal fracture seen in the figure varies in length with misorientation of the dicing blade. The groove width appears larger and the damage region widens with misorientation of the blade. A measurement of the groove width of (1 0 0) n-type silicon ranged from 5.5×10^{-2} mm at 0°, to 7.25×10^{-2} mm at 20°. Fig. 5 shows scanning electron micrographs of the sidewalls, and the bottom of a single groove after etching. The groove sidewalls show evidence of median cracks that result from individual diamond contacts with the silicon surface, as well as plastic deformation. The bottoms of the grooves show that median cracks propagate down and away from the contact zone. This groove surface morphology had been previously observed by Kim [10] in a study of dicing of silicon as a function of lubricating fluids and isothermal temperature.

Optical micrographs of the bevel region (Fig. 6), shows evidence of cracking that surrounds the tip of the groove. Referring to the micrographs of the grooved specimen in the ⟨1 1 0⟩ of the (1 1 1) n-type silicon, typical cracks lie along the cleavage direction and occasionally follow the chevron cracks formed during dicing. These results show that the cutting orientations play an important role in the generation, propagation, and intersection of cracks.

Figure 4 Optical micrographs of the (1 0 0) surface abraded by various crystallographic cutting directions. (a) [1 1 0], (b) 10°, (c) 20°, (d) 30°.

The resistivity of the groove and bevel region, calculated as a percent change $[(\rho - \rho_0)/\rho_0]$ is shown in Figs 7 and 8, where ρ and ρ_0 are the resistivities of the damaged and undamaged specimens, respectively. The data show that the resistivity varies along the groove even though each groove was made to be of the same depth. This implies that the damage depth changes and is statistically variable along the length of the groove. The variability in the resistivity is larger for the (1 0 0) than the (1 1 1). The percent change in resistivity of both (1 0 0) and (1 1 1) samples increases as a function of the angle of misorientation. If the changes in resistivity are averaged along the groove length, then the resistivity increases from $\approx 4\%$ to $\approx 10\%$ for the (1 0 0) and from $\approx 6\%$ to $\approx 8\%$ for the (1 1 1).

As the probes were translated along the bevel, the resistivity decreased and an extrapolation to zero groove depth may be used as a measure of the subsurface damage due to misorientation alone. Fig. 9 shows

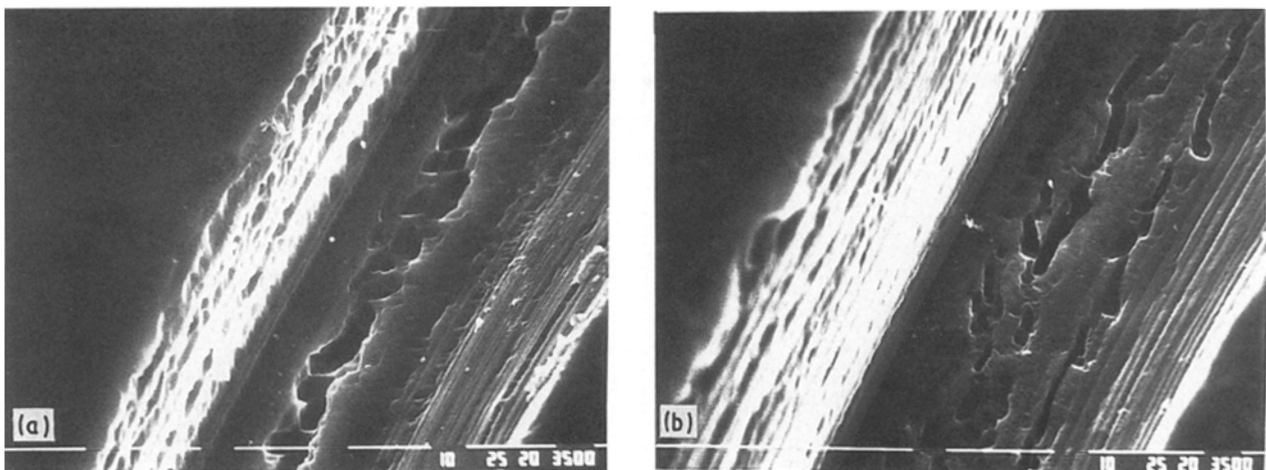

Figure 5 Scanning electron micrographs of the etched side walls, and bottom of a single groove. (a) 0°, (b) 10°, (c) 20°, (d) 30°.

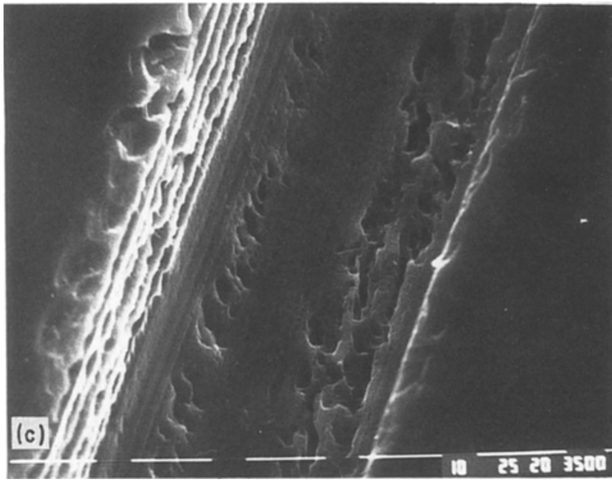

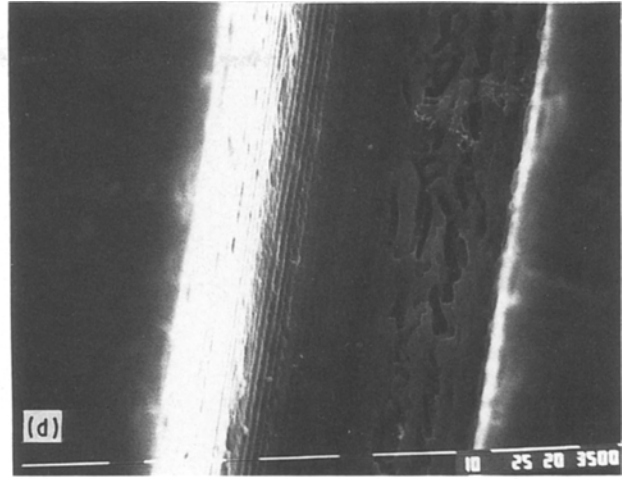

Figure 5 Continued.

the variation of the resistivity along the bevel for the (1 0 0) and Fig. 10 for the (1 1 1). As can be seen, the change in resistivity decreases to zero as the probes are traversed toward the bevel tip. The intersection of each line with the horizontal axis is an indication of the subsurface damage depth as denoted by D_0, D_1, D_2, and D_3 in Fig. 9. These results indicate that the largest subsurface damage occurs at a misorientation of 20°. The damage zone depth as obtained from this extrapolation is plotted against blade misorientation in Fig. 11. This figure shows that the damage zone size is a maximum of 0.122 mm for the (1 0 0) and 0.186 mm for the (1 1 1) specimens, respectively for the blade misorientation of 20°. These results are consistent with the study of Danyluk *et al.* [11], in which the relative change in resistivity was found to increase with temperature as well as with doping level. These workers observed that the damage induced by the single diamond scratch in (1 0 0) n-type silicon scratch is proportional to the resistivity across the scratched region and, plastic flow will induce a smaller change in resistivity than brittle fracture.

Our experimental results show that the size and/or resistivity of the damaged region underneath the

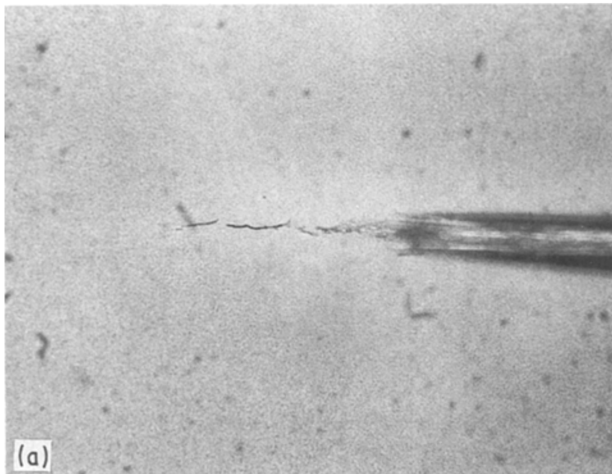

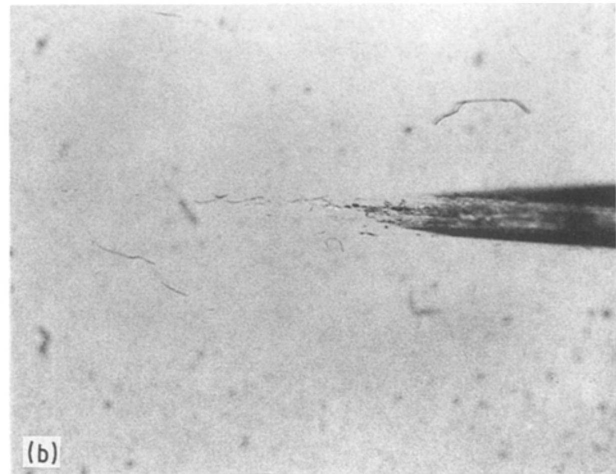

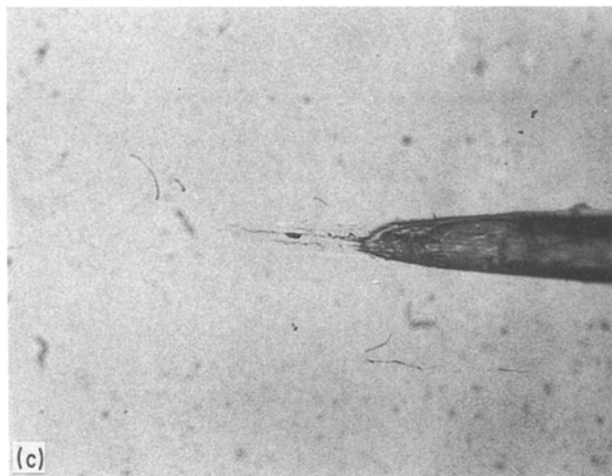

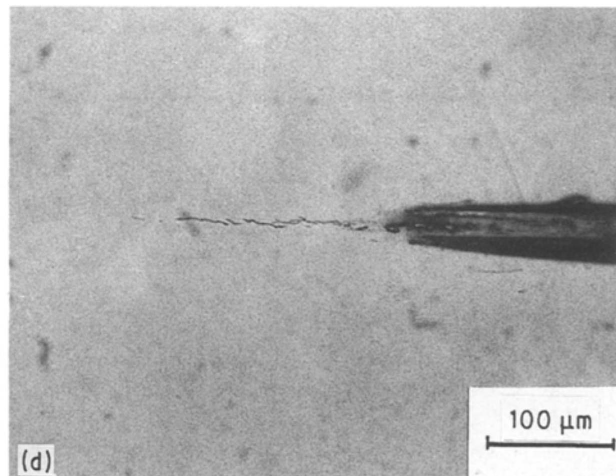

Figure 6 Optical micrographs of the bevelled region found in the (1 1 1) surface microcracks surrounding the tip of the groove.

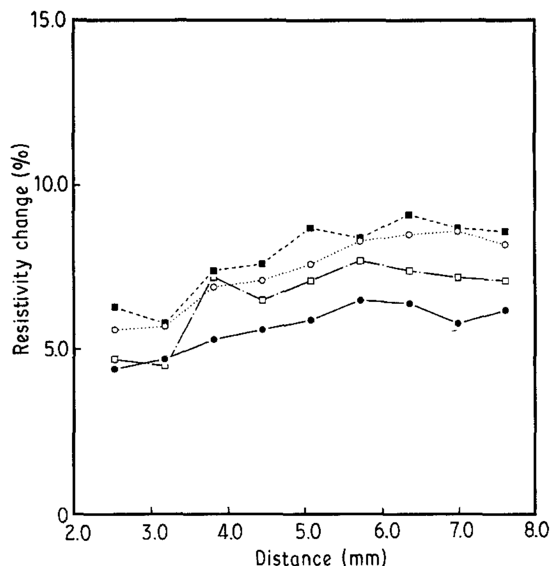

Figure 7 The change in resistivity (%) plotted against distance along the groove (mm) as a function of the blade misorientation for the (1 1 1) sample. (● [1 $\bar{1}$ 1] direction, ○ 10°, ■ 20°, □ 30°)

groove varies with the crystallographic cutting orientation. The resistivity of the damaged layer will be related to the geometry of the groove and the size and geometry of the subsurface damage. The resistivity change may be described [11] with a parameter, M, as

$$M = \frac{\rho - \rho_0}{\rho_0} = \frac{b^2}{d^2}\left(1 - \frac{2\sigma_2}{\sigma_1}\right)$$

where d is the probe spacing, and σ_1 and σ_2 the conductivity of the undamaged and damaged silicon wafer, respectively, and b the depth of the groove. Since d and σ_1 are constant, the change in resistivity depends on b and σ_2, the size and conductivity of the damage zone respectively. It is not possible, from these experiments alone, to determine which of the parameters is the more significant to determining M until the subsurface damage is characterized by microscopy. This work is continuing and will be reported shortly.

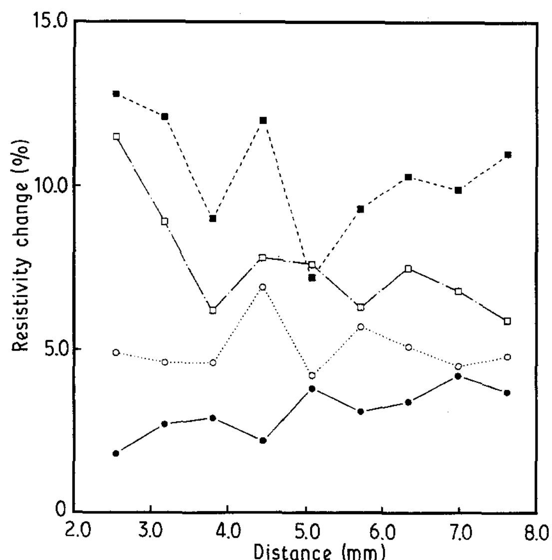

Figure 8 The change in resistivity (%) plotted against distance along the groove as a function of blade misorientation for the (1 0 0) sample. (Symbols as in Fig. 7)

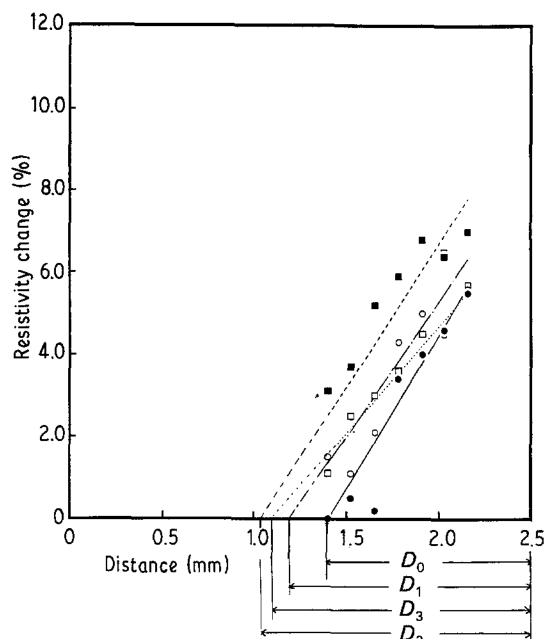

Figure 9 The change in resistivity (%) plotted against distance along the bevel (mm) as a function of blade misorientation for the (1 0 0) sample. (Symbols as in Fig. 7)

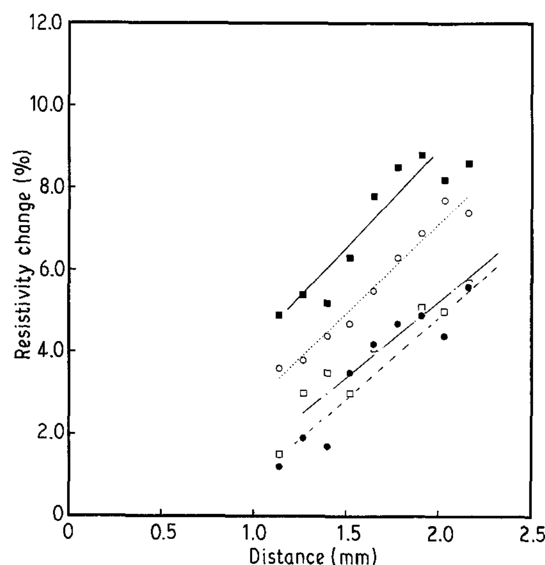

Figure 10 The change in resistivity (%) plotted against the bevel (mm) as a function of blade misorientation for the (1 1 1) sample. (Symbols as in Fig. 7)

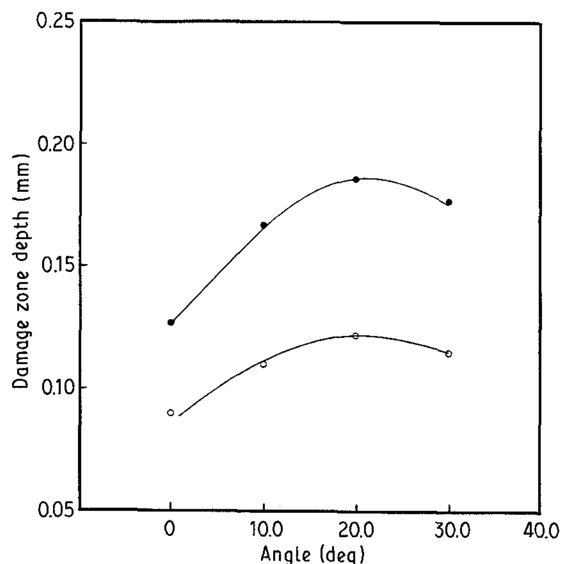

Figure 11 Damage zone size (mm) as a function of the blade misorientation (degrees). (○ (1 1 1) n-type, ○ (1 0 0) n-type)

Acknowledgements
This work was supported by the National Science Foundation Grant No. MSM-8714491. We thank Dr Jorn Larsen-Basse for this support and interest in this work. The silicon wafers were supplied by the Monsanto Electronic Materials Company and the dicing blades were obtained from Ernst Winter and Son, Inc. We thank these organizations for the support. Additional thanks are extended to James Tomei, John Gramsas, Ji Hong Ahn, Hae Woong Park, Dong Soo Park, and Soo Wohn Lee.

References
1. T. M. BUCK and R. L. MEEK, Silicon Device Processing, NBS Special Publication 337: (1970) pp. 419–430.
2. H. FRANK, *Solid State Electron.* **9** (1969) 609.
3. S. DANYLUK and R. REAVES, *Wear* **77** (1982) 81.
4. R. L. MEEK and M. C. HUFFSTUTTLER, *J. Electrochem. Soc.* **116** (1980) 893.
5. T. S. KUAN, K. K. SHIH, J. A. VANVECHTEN and W. A. WESTDORP *J. Electrochem. Soc.* **127** (1980) 1387.
6. C. J. GALLAGHER, *Phys. Rev.* **88** (1952) 772.
7. D. S. LIM and S. DANYLUK, *J. Mater. Sci.* **23** (1952) 2607.
8. S. W. LEE, PhD Thesis, University of Illinois at Chicago (1986).
9. American Society for Testing and Materials: "1977 Annual Book of ASTM Standard", ANSI/ASTM (1977) pp. f84-73.
10. J. M. KIM, PhD Thesis, University of Illinois at Chicago (1986).
11. D. DANYLUK, S. W. LEE, G. H. AHN and A. KAHN, *J. Appl. Phys.* **63** (1988) 4568.

Received 22 June
and accepted 1 December 1989